Mg-dechelatase is involved in the formation of photosystem II but not in chlorophyll degradation in *Chlamydomonas reinhardtii*

Author Affiliations:
Ying Chen, Yousuke Shimoda, Makio Yokono, Hisashi Ito, Ayumi Tanaka
Institute of Low Temperature Science, Hokkaido University, Sapporo 060-0819, Japan

Corresponding Author:
Hisashi Ito
Institute of Low Temperature Science, Hokkaido University, Sapporo 060-0819, Japan
Tel +81-11-706-5493
E-mail: ito98@lowtem.hokudai.ac.jp

Running title: Mg-dechelatase and photosystem II formation

Keywords: STAY-GREEN | Mg-dechelatase | photosystem II formation | chlorophyll degradation | pheophytin *a*

SUMMARY

The STAY-GREEN (*SGR*) gene encodes a Mg-dechelatase that catalyzes the conversion of chlorophyll (Chl) *a* to pheophytin (Pheo) *a*. This reaction is the first and most important regulatory step in the chlorophyll degradation pathway. Conversely, Pheo *a* is an indispensable molecule in photosystem (PS) II, suggesting the involvement of SGR in the formation of PSII. To investigate the physiological functions of SGR, we isolated Chlamydomonas *sgr* mutants by screening an insertion-mutant library. The *sgr* mutants had reduced maximum quantum efficiency of PSII (Fv/Fm) and reduced Pheo *a* levels. These phenotypes were complemented by the introduction of the Chlamydomonas *SGR* gene. Blue-native polyacrylamide gel electrophoresis and immunoblotting analysis showed that although PSII levels were reduced in the *sgr* mutants, PSI and light-harvesting Chl *a*/*b* complex levels were unaffected. Under nitrogen starvation conditions, Chl degradation proceeded in the *sgr* mutants as in wild type, indicating that Chlamydomonas SGR is not required for Chl degradation and primarily contributes to the formation of PSII. In contrast, in the Arabidopsis *sgr* triple mutant (*sgr1 sgr2 sgrL*), which completely lacks SGR activity, PSII was synthesized normally. These results suggest that the Arabidopsis SGR participates in Chl degradation, while the Chlamydomonas SGR participates in PSII formation in spite of the same catalytic property.

INTRODUCTION

Photosynthesis fixes CO_2 into sugar, upon which most living organisms depend. Two photosystems (PSs), PSI and PSII, are responsible for the initial processes of photosynthesis, such as harvesting light energy, driving electron transfer and forming proton gradients. PSs are large complexes consisting of proteins, chlorophylls (Chls), carotenoids and other prosthetic groups such as quinones and iron-sulfur centers (Nelson and Junge, 2015). The PSII core complex consists of approximately 35 Chls and more than 20 intrinsic and extrinsic proteins (Umena *et al.*, 2011). In green plants, the light-harvesting Chl *a*/*b* complex (LHCII) associates with PSII core complexes to form a large supercomplex that is more than 1000 kDa in size (Drop *et al.*, 2014, Nosek *et al.*, 2017). The regulation and molecular mechanisms of PSII formation have been extensively studied in recent years using genetic and biochemical approaches (Uniacke and Zerges, 2007, Rengstl *et al.*, 2011). The first step of PSII formation is the assembly of Chl with an apoprotein, and a terminal Chl biosynthesis enzyme, Chl synthase, has been suggested to be part of the assembly complex (Chidgey *et al.*, 2014). The next step of PSII formation is the assembly of D1, D2 and cytochrome b_{559} to form a reaction center (RC47) to which CP47 associates. CP43 incorporates into RC47 and is followed by an association of extrinsic oxygen-evolving complexes. Finally, in green plants, the PSII core complex dimerizes and binds to LHCII to form PSII supercomplexes (Komenda *et al.*, 2012, Nickelsen and Rengstl, 2013, Plochinger *et al.*, 2016).

The Chl composition of the reaction center complex (D1/D2 heterodimer) is different from that of other light-harvesting complexes because only the reaction center complex contains pheophytin *a* (Pheo *a*) in addition to Chl *a*, suggesting that supply of Pheo *a* contributes to the formation of the reaction center complex. However, the impact of Pheo *a* synthesis on the formation of PSII has never been addressed because the manner of production of Pheo *a* has long been unknown (Hortensteiner, 2013, Shimoda *et al.*, 2016). The Mg in Chl is spontaneously released under acidic conditions (Saga *et al.*, 2013), which led to the hypothesis that Pheo *a* is nonenzymatically produced from Chl *a* under such conditions (Christ and Hortensteiner, 2014). Recently, we identified a Mg-dechelatase, STAY-GREEN (*SGR*), in Arabidopsis (Shimoda *et al.*, 2016) and Chlamydomonas (Matsuda *et al.*, 2016) that removes Mg and converts Chl *a* to Pheo *a*. These studies clearly show that Pheo *a* is not spontaneously produced but is enzymatically synthesized.

There are three hypotheses for the production of Pheo *a* in PSII formation. The first is that it is produced by SGR; the second is that it is produced by an unidentified Mg-dechelatase, and the third is that it is formed in the PSII reaction center. To examine these possibilities, we used Chlamydomonas *sgr* mutants because they can heterotrophically grow without PSII. These *sgr* mutants had low PSII level, while PSI and LHCII levels were unchanged which is different from Arabidopsis *sgr* triple mutant (*sgr1 sgr2 sgrL*). Based on these results, we discuss the role of SGR in the formation and degradation of PSs from an evolutionary viewpoint.

RESULTS

Isolation of Chlamydomonas *sgr* Mutants and Analysis of Phenotypes

First, we hypothesized that if Pheo *a* is not supplied, PSII cannot be formed, resulting in a reduced Fv/Fm ratio. To isolate Mg-dechelatase mutants, a mutant library was generated using insertional DNA mutagenesis. Mutagenized Chlamydomonas cells were grown on agar plates under low light conditions to avoid photodamage. For the first screening, we determined the Fv/Fm ratios of approximately 80,000 Chlamydomonas mutants using a Chl fluorometer imaging system (FluorCam). Colonies with low Fv/Fm ratios were selected, although the sizes of these colonies were highly variable, and they were cultured in liquid medium containing acetate. For the second screening, Fv/Fm ratios were determined using a PAM Chl fluorometer, and 200 mutants with low Fv/Fm ratios (below 0.5) were isolated. The DNA regions in 150 of these mutants were flanked by the inserted DNAs were identified using thermal asymmetric interlaced (TAIL)-PCR. Assuming a large genomic DNA deletion of following the DNA insertion (Tanaka *et al.*, 1998) , we estimated that these 150 mutants could be classified into 60 groups, with 1–7 independent mutants in each group. Among these groups, we identified one group within which the *SGR* gene was expected to be deleted. We confirmed the deletion of *SGR* in two of these mutants using PCR analysis (Fig. S1), and we used the same two *sgr* null mutants for our experimental analysis.

We examined the effect of light intensity on the Fv/Fm ratio. Under normal light condition (80 μmol photons m^{-2} s^{-1}, NL80), the WT Fv/Fm ratio was approximately 0.80 but the *sgr* mutants exhibited low Fv/Fm ratios (Fig. 1*A*). To confirm that the mutant phenotype was caused by the deletion of the *SGR* gene, the intact Chlamydomonas *SGR* gene was introduced into the *sgr* mutant genomes. The Fv/Fm ratios of two complementation lines were restored to the WT level (Fig. 1*A*), indicating that the low Fv/Fm phenotype was caused by the deletion of the *SGR* gene. Under high light conditions (250 μmol photons m^{-2} s^{-1}, HL250), the Fv/Fm ratios were decreased similarly in both the WT and *sgr* mutants. Interestingly, the Fv/Fm ratios of the *sgr* mutants were still reduced under extremely low light conditions (1 μmol photons m^{-2} s^{-1}, LL1) (Fig. 1*A*). This result indicates that the low Fv/Fm ratios found in the *sgr* mutants are not caused by photoinhibition.

Next we examined the response of the Chlamydomonas cells to strong light conditions (750 μmol photons m^{-2} s^{-1}, SL750). Stationary phase cells grown under NL80 light were exposed to SL750 light. The WT Fv/Fm ratios were reduced with strong light treatment and remained at approximately 0.2. However, the Fv/Fm ratios of the *sgr* mutants were rapidly reduced to 0 and did not recover (Fig. 1*B*), indicating that the mutant cells died under strong light conditions.

We examined the effect of the *SGR* mutation on the growth rate in the presence (TAP medium) or absence (HSM medium) of a carbon source. Using either media, the *sgr* mutants had reduced growth rates compared to the WT under normal light conditions, while the complemented lines had growth

rates similar to the WT (Fig. S2*A*). The *sgr* mutants could still grow photoautotrophically (Fig. S2*B*), although the Fv/Fm ratios were reduced, indicating that functional PSII is still formed in the *sgr* mutants.

Accumulation of Pheo *a*

Previously, we showed that Chlamydomonas SGR catalyzes the conversion of Chl *a* to Pheo *a* (Matsuda *et al.*, 2016). One possible reason for the reduced Fv/Fm ratio is a limited supply of Pheo *a* for PSII formation. We measured the pool of Pheo *a* using high performance liquid chromatography (HPLC). The Pheo *a*/Chl was approximately 0.09 in the WT during the very early growth phase (Fig. 2). This value is largely consistent with a previous report, which found a Chlamydomonas Chl/Pheo *a* ratio of 100 (Maroc and Tremolieres, 1990). The levels of Pheo *a* in the *sgr* mutants were approximately 60% of that of the WT in the early growth phase. The introduction of the *SGR* gene into the *sgr* mutants increased the Pheo *a* level beyond that of the WT and was accompanied by an increase in the Fv/Fm ratio (Fig. 1). This result indicates that PSII is not efficiently formed in the *sgr* mutants because of the limited supply of Pheo *a*. The Pheo *a* level was increased as the culture period increased. The reason for this result is not clear, but it could be associated with partial Chl degradation or cell death during the later stages of culture.

PSII and PSI levels in Chlamydomonas *sgr* mutants

Fluorescence and pigment analysis suggested that there was a PSII formation defect in the Chlamydomonas *sgr* mutants. To examine whether the PSs were properly formed in the mutants, the PSs were analyzed using blue-native polyacrylamide gel electrophoresis (BN-PAGE). Using WT cells, seven major and several minor green bands were resolved on the gel (Fig. 3*A*). To identify the major green bands, the low temperature fluorescence spectra of bands 1–5 were measured (Fig. S3). Although Coomassie brilliant blue quenches the LHCII excitation energy (Yokono *et al.*, 2015), PSI and PSII fluorescence can be measured by using green gel pieces. In the WT, bands 1, 2 and 3 had similar fluorescence spectra, each with a peak at approximately 690 nm that is characteristic of a PSII spectrum. Band 4 exhibited PSI fluorescence and had a small PSII peak. Band 5 also exhibited fluorescence peaks of both PSs. This band could contain PSI-LHCI and the PSII-dimer, which are known to co-migrate on the gel (Takabayashi *et al.*, 2011a). These PSs were confirmed by SDS-PAGE of the individual green bands (Fig. 3*B*, Fig. S4).

The intensities of bands 1, 2, and 3 from the *sgr* mutants were reduced in comparison with those of WT. Fluorescence at approximately 720 nm in these three bands of the mutant could be derived from contaminated PSI. The PSII fluorescence was dominant in band 4 of the *sgr* mutant which is slightly different from the WT. Band 5 of the *sgr* mutants had a fluorescent peak at 720 nm and a very low or lack of a peak corresponding to PSII. These results clearly indicate that the PSII levels are reduced in the *sgr* mutants (Fig. S5). The intensities of the PSI and LHCII bands were not particularly different between the *sgr* mutants and WT. Low temperature fluorescence spectra

measurements of the cells also detected reduced PSII levels in the *sgr* mutants (Fig. S5). In order to determine the level of PSI, we measured the Chl/P700 ratio using spectroscopic method (Table.S1). The Chl/P700 ratio of the WT and the Chlamydomonas *sgr* mutant was 310 and 240, respectively, indicating that the level of PSI per Chl is slightly high in the mutant. The levels of the individual proteins from the PSs were examined using immunoblotting (Fig. 4). In the *sgr* mutants, most of the PSII proteins were reduced by 75% or more in comparison with the WT. The levels of the PSI proteins and LHCII proteins were not particularly different between the *sgr* mutants and the WT. These results also indicate that PSII is preferentially reduced in the *sgr* mutants.

SGR was not associated with Chl degradation in Chlamydomonas

SGR catalyzes the first step of Chl degradation in land plants and Chl degradation was delayed in the *sgr* mutants (Park *et al.*, 2007). The contribution of SGR to the Chl degradation was examined in Chlamydomonas. Instead of senescence, Chl degradation was induced by nitrogen (N) starvation (Fig. 5*A*). When the cells were transferred to nitrogen-free medium, the Chl content transiently increased during the first day and then decreased. After four days of N-starvation, the Chl degradation rate slowed, which is consistent with a previous study (Schmollinger *et al.*, 2014). The Chl degradation rates in the *sgr* mutants and the WT were nearly the same (Fig. 5*B*). It has been reported that chlorophyll is more rapidly degraded under nitrogen deprivation under photoautotrophic conditions than under mixotrophic conditions in Chlamydomonas (Schulz-Raffelt *et al.*, 2016). When Chlamydomonas was cultured with high CO_2 (5% CO_2 in air) under nitrogen starvation in TP media for 4 days, 65 and 70-75% of the chlorophyll was degraded in the WT and the *sgr* mutants, respectively (Fig. S6). These results suggest that Chlamydomonas SGR (CrSGR) is not involved in chlorophyll degradation or some other Mg-dechelatases compensate for the loss of SGR.

NON-YELLOW COLORING1 (NYC1), pheophorbide *a* oxygenase (PaO) and SGR are responsible for Chl degradation, and the expression of these genes is up-regulated during leaf senescence (Sakuraba *et al.*, 2012b). Quantitative real-time polymerase chain reaction (qRT-PCR) results showed that after three days of nitrogen starvation the mRNA expression levels of *NYC1* and *PaO* both increased (Fig. 5*C*). These results suggest that these two genes are also involved in Chl degradation in Chlamydomonas. However, the *SGR* mRNA expression level was reduced by nitrogen starvation (Fig. 5*C*). This reduced *SGR* expression is substantially different from Arabidopsis, in which the *SGR* mRNA expression level is up-regulated during Chl degradation (Sakuraba *et al.*, 2012b). These results indicate that SGR is not associated with Chl degradation in Chlamydomonas.

SGR was not involved in PSII formation in Arabidopsis

It had previously been unclear whether SGR is involved in PSII formation in Arabidopsis, because a *SGR* knock-out mutant was unavailable. Arabidopsis has three *SGR* genes: *SGR1*, *SGR2* and *SGRL*. To elucidate the physiological role of SGR, we constructed an Arabidopsis *sgr* triple mutant (*sgr1*

sgr2 sgrL). The triple mutant germinated and developed like the WT (Fig. 6*A*). PSII protein levels (Fig. 6*B*) and the Fv/Fm ratio (Fig. 6*C*) in the developing tissues were the same between the *sgr* triple mutant and WT, indicating that SGR is not involved in PSII formation in Arabidopsis. Consistent with these results, the level of Pheo *a* did not differ greatly between the WT and the *sgr* triple mutant before senescence (Table.S2). Next, we examined the impact of the complete deletion of the *SGR* genes on chlorophyll degradation. Although Chl degradation was observed in the WT and the *sgr* triple mutant, a larger amount of Chl was retained in the mutant compared to the WT during natural senescence (Fig. 6*D*). Chl and carotenoids were also retained at higher levels in the mutant during dark-induced senescence (Table.S2). The BN-PAGE analysis (Fig. 6*E*) shows that the photosystems and light-harvesting complexes were retained in the mutant, while these complexes almost completely disappeared in the WT. These experiments indicate that SGR plays a crucial role in chlorophyll degradation in Arabidopsis.

The Arabidopsis *sgr* mutant phenotype was rescued by *CrSGR*

A previous study showed that CrSGR has the same catalytic properties as Arabidopsis SGR (AtSGR)1and that transiently expressed *CrSGR* induced chlorophyll degradation in Arabidopsis (Matsuda *et al.*, 2016). In this study, *CrSGR* was constitutively expressed in an Arabidopsis *sgr* triple mutant using 35S promoter (CrSGR-35S) or an Arabidopsis native promoter (2 kbp upstream from the translation start site of *AtSGR1*) (CrSGR-N) (Fig. S7*A*). The *sgr* triple mutant exhibited the stay green phenotype during dark-induced senescence, while the leaves of the WT turned yellow after dark incubation (Fig. S7*B*). The leaves of CrSGR-N turned only slightly yellow after dark incubation. Some leaves of the CrSGR-35S plants were yellow before senescence and turned slightly yellow after dark incubation. Under natural senescence (Fig. S7*C*), the *sgr* triple mutant showed the stay green phenotype, while the WT turned yellow at the senescence stage. These experiments indicate that *CrSGR* at least partly rescues the *sgr* phenotype of Arabidopsis. In these experiments, we had to select transgenic lines with a low expression level of *CrSGR* because if *SGR* is highly expressed, all the chlorophyll is degraded, and the plant cannot survive, which could be the reason why the *sgr* mutant phenotype was not completely rescued by *CrSGR*. In summary, it appears that SGR is associated with different physiological processes in Arabidopsis and Chlamydomonas, despite having the same catalytic function in each species.

DISCUSSION

Chlamydomonas *sgr* mutants had low Fv/Fm ratios (Fig. 1*A*). These low Fv/Fm ratios were not caused by photoinhibition or light stress because Chlamydomonas cells grown under extremely low light conditions also exhibited similar Fv/Fm ratio to those grown under normal light conditions. One possible mechanism for the low Fv/Fm ratio is a defect in the assembly of PSII (Sirpio *et al.*, 2008, Zhang *et al.*, 2010). In support of this mechanism, the levels of PSII and its components,

including D1, D2, CP43 and CP47, were extremely low in the Chlamydomonas *sgr* mutants (Fig. 4). Based on these experiments, we concluded that, in Chlamydomonas, SGR contributes to the formation of PSII by supplying Pheo *a*. However, the Fv/Fm ratio was approximately 0.4 (Fig. 1*A*) but not 0. Therefore, PSII formation was not completely blocked in the Chlamydomonas *sgr* mutants. Consistent with these results, Pheo *a* accumulated in the Chlamydomonas *sgr* mutants to approximately 60% of the levels found in the WT (Fig. 2). The Pheo *a* in the *sgr* mutant could be formed by other mechanisms. Although the Pheo *a* levels in the Chlamydomonas *sgr* mutants were 60% of the WT, the levels of the D1 protein were less than 25% of the WT (Fig. 4). This result suggests that Pheo *a* is synthesized by other mechanisms and is not efficiently used for PSII formation. The Pheo *a*/Chl ratio determined using HPLC in this study is different from the value determined using an optical method (Guenther *et al.*, 1990), suggesting the accumulation of nonfunctional Pheo *a*. The Pheo *a*/Chl ratios of the Chlamydomonas *psb*D mutant, which does not accumulate PSII (Erickson *et al.*, 1986), and the WT were between 0.005-0.007 and 0.008-0.010, respectively (Fig. S8), indicating that the mutant lacking PSII accumulated Pheo *a* at a similar level of the *sgr* mutant. The existence of the Pheo *a* unbound to PSII could be one of the reason for the discrepancy between D1 and Pheo *a* content of the Chlamydomonas WT and the *sgr* mutants.

The conversion of Chl *a* to Pheo *a* is the first step of Chl degradation (Hortensteiner, 2006), and *SGR* is up-regulated during leaf senescence (Park *et al.*, 2007). The *sgr* mutants of various land plants have a delayed Chl-degradation phenotype (Cha *et al.*, 2002, Armstead *et al.*, 2007, Barry *et al.*, 2008, Zhou *et al.*, 2011). However, the Chl degradation rates in Chlamydomonas were not particularly different between the *sgr* mutants and the WT in this study (Fig. 5*A*, 5*B*, Fig. S5). Interestingly, *SGR* was not up-regulated during N starvation as the Chl began to be degraded, unlike other Chl-degradation enzymes, including PaO and NYC1. This result suggests that SGR is not involved in Chl degradation in Chlamydomonas (Fig. 5*C*). However, it should be noted that the substrates of pheophytinase (PPH) and PaO in the Chl-degradation pathway are Pheo *a* and pheophorbide *a*, respectively (Pruzinska *et al.*, 2003, Schelbert *et al.*, 2009). These molecules have no central Mg. Therefore, in Chlamydomonas, the Mg molecules must have been removed before the reactions that are catalyzed by PPH and PaO. This phenomenon can only be explained by the existence of a second Chl degrading Mg-dechelatase in Chlamydomonas.

The physiological functions of SGR have been extensively studied in vascular plants (Bell *et al.*, 2015, Sakuraba *et al.*, 2015, Qian *et al.*, 2016). Without exception, the *sgr* mutant had a strong stay-green phenotype, which is consistent with SGR catalyzing the first and committed step of Chl degradation. There are three *SGR* genes in the Arabidopsis genome: *SGR1*, *SGR2* and *SGRL* (Sakuraba *et al.*, 2015, Shimoda *et al.*, 2016). *SGR1* and *SGR2* are expressed during senescence, and the *sgr1*/*sgr2* double mutant shows a strong stay-green phenotype (Wu *et al.*, 2016). These results indicate that SGR1 and SGR2 are responsible for Chl degradation during senescence. By contrast,

SGRL is primarily expressed in green tissues and is significantly down-regulated in leaves undergoing natural and dark-induced senescence (Rong *et al.*, 2013) (Jiang *et al.*, 2007, Ren *et al.*, 2007, Pilkington *et al.*, 2012). Although the *SGRL* expression pattern suggests its involvement in PSII formation, the PSII level and the Fv/Fm ratio of the Arabidopsis *sgr* triple mutant (*sgr1 sgr2* and *sgrL*) were the same as those of the WT (Fig. 6*C*), suggesting that SGR does not contribute to PSII formation in Arabidopsis.

The formation of PSII and its repair cycle are important processes that are regulated by many factors (Nickelsen and Rengstl, 2013, Theis and Schroda, 2016). In these processes, the supply of Pheo *a* must be strictly regulated: if Pheo *a* is limited, the PSII level will be reduced, and if Pheo *a* is in present in excess, it is toxic to cells and a waste of Chl *a*. It might be difficult to supply an appropriate amount of Pheo *a* by spontaneous Mg release from Chl *a* under acidic conditions. Therefore, another Mg-dechelatase is likely to be associated with PSII formation in Arabidopsis.

In this study, we show that the physiological function of SGR is different between Arabidopsis and Chlamydomonas. The Arabidopsis SGR is involved in Chl degradation, while the Chlamydomonas SGR contributes to PSII formation. In Arabidopsis, SGR and NYC1 are associated with the degradation of Chl in the LHC and core antenna complexes, respectively. The question arises as to why SGR is not also involved in Chl degradation in Chlamydomonas. Green plants are divided into two groups, chlorophytes and streptophytes. Chlorophytes initially evolved in the deep sea (Leliaert *et al.*, 2011), and early branching chlorophytes have Chl *b* not only in the LHC but also in the core antenna complexes (Kunugi *et al.*, 2016). As shown previously, SGR does not extract Mg from Chl *b* (Shimoda *et al.*, 2016), suggesting that SGR cannot efficiently degrade Chl in the core antenna complexes when they contain Chl *b*. This assumption is consistent with the result that Arabidopsis transgenic plants with core antennae containing Chl *b* have a stay-green phenotype that is indicative of delayed Chl degradation including both Chl *a* and Chl *b* (Sakuraba *et al.*, 2012a). Although Chlamydomonas does not have Chl *b* in its core antenna complexes, its progenitor had Chl *b* in the core antenna complexes (Kunugi *et al.*, 2016). The progenitor would not have been able to use SGR for Chl degradation for above reasons and might use another system or mechanism. This characteristic of the progenitor is likely to have been inherited by Chlamydomonas. By contrast, Chl *b* is not present in the core antenna complexes of streptophytes, including Arabidopsis, and SGR can degrade all the Chl in the core antennae, which might be one of the reasons why SGR has different physiological functions between Arabidopsis and Chlamydomonas. It should be noted that AtSGR1 and CrSGR catalyze the same reaction that converts Chl *a* to Pheo *a* but not chlorophyllide *a* to pheophorbide *a* (Matsuda *et al.*, 2016). In addition, *CrSGR* partly complemented an Arabidopsis *sgr* triple mutant (Fig. S7) and transiently expressed *CrSGR* in Arabidopsis induced chlorophyll degradation (Matsuda *et al.*, 2016). These results indicate that the enzymatic properties between AtSGR and CrSGR are identical, but the physiological functions are different. The difference in the

physiological function of the two enzymes could be caused by other mechanisms such as the location of the enzyme.

This study suggests that there is another unidentified Mg-dechelatase in both Chlamydomonas and Arabidopsis. Photosynthetic organisms other than green plants, such as red algae and cyanobacteria, do not possess *SGR*, but they still have PSII and degrade Chl. Therefore, it is likely that there is an as-yet unidentified Mg-dechelatase that is associated with PSII formation and Chl degradation in these organisms. This unidentified Mg-dechelatase could also be a candidate for the second Mg-dechelatase in green plants.

Materials and Methods

Materials and cultivation conditions. *Chlamydomonas reinhardtii* (CC-1618 cw15 arg7 mt-, CC-4385; PsbD deletion mutant) was grown photomixotrophically (TAP media) or photoautotrophically (HSM media). Cultures of 40 mL were shaken in 100 mL Erlenmeyer flasks at 120 rpm under continuous fluorescent light (1, 80 or 250 μmol photons m^{-2} s^{-1}) at 25 °C. For strong light treatment, stationary phase Chlamydomonas cells cultivated at 80 μmol photons m^{-2} s^{-1} were exposed to 750 μmol photons m^{-2} s^{-1}. Nitrogen starvation of the Chlamydomonas culture was described previously (Sharma *et al.*, 2015).

Arabidopsis thaliana (Columbia ecotype) was grown as described previously (Shimoda *et al.*, 2016). *sgr* triple mutants were obtained by crossing mutants lacking *SGR1* (Ren *et al.*, 2007), *SGR2* (SALK_003830C) and *SGRL* (SALK_084849). The mutations were confirmed using PCR-based genotyping and genomic DNA sequencing. The *sgr2* and *sgrL* mutants were obtained from the Arabidopsis Biological Resource Center.

Construction of the mutant library. The mutant library was generated by DNA insertional mutagenesis using the pSI-103 vector (Chlamydomonas Resource Center) as described previously (Tanaka *et al.*, 1998). The strategy for isolating *sgr* mutants is described in the Results. To identify a DNA region flanked by the inserted DNA, TAIL-PCR was conducted as previously described (Matsuo *et al.*, 2008).

Complementation of the Chlamydomonas *sgr* mutant. Chlamydomonas SGR cDNA for the CrSGR complemented line was prepared by PCR using specific primers for SGR (*Cr_SGR*). The amplified fragments were introduced into the pChlamy_1 vector (Invitrogen) between the *Nco*I and *Not*I sites. The *Nco*I site was created by modifying the original start codon. Chlamydomonas-complemented cells were screened by measuring the Fv/Fm ratio and confirmed using genomic PCR (Fig. S1), and the primer pairs are listed in Table.S3.

Complementation of the Arabidopsis *sgr* mutant. CrSGR with the Arabidopsis SGR1 transit peptide was prepared as previously described (Matsuda et al., 2016). This fragment was introduced into the Gateway entry vector pENTR4 Dual and then introduced into the Gateway-compatible inducible vector pEarleyGate 100. The construct was introduced into Agrobacterium tumefaciens (strain GV3101) and transformed into the Arabidopsis *sgr1 sgr2 sgrl* mutant. Transgene expression was stably driven using the 35S promoter. The promoter of Arabidopsis SGR1 (2 kbp) was amplified from Arabidopsis genomic DNA using specific primer sets (AtSGR1_promoter) and fused with the Chlamydomonas SGR with the Arabidopsis SGR1 transit peptide. This construct was introduced into Arabidopsis using pEarleyGate 301 as described above. The transformants were confirmed by genomic DNA PCR using the specific primer sets (CrSGR_T) to amplify CrSGR using the terminator fragments.

Measurement of the Fv/Fm ratio. Fv/Fm was measured using a PAM-2500 (Walz) chlorophyll fluorometer after 10 min of dark acclimation.

HPLC analysis of the pigment. Chlamydomonas cells were harvested by centrifugation at 22,500 × *g* for 1 min and resuspended in 50 μL of water and 200 μL of acetone. Arabidopsis developmental stage fresh and seven days dark-incubated leaves were ground in in 20-fold pure acetone and stored in -20 °C. This solution was mixed vigorously for 1 min and centrifuged at 22,500 × *g* for 10 min. The supernatant (20 μL) was subjected to HPLC using a RF20A fluorescence detector and a SPD-M10A diode array detector (Shimadzu). Pigment separation was performed using a symmetry C8 column (150 mm in length and 4.6 mm in inner diameter; Waters), as previously described (Shimoda *et al.*, 2016). Calibration curves of known pigments were constructed to quantify the chlorophyll and pheophytin.

BN-PAGE analysis and silver staining. Chlamydomonas cells were collected at the logarithmic growth phase using centrifugation at 7,000 × *g* for 5 min at 4 °C and resuspended in buffer containing 50 mM imidazole/HCl (pH 7.0), 20% (w/vol) glycerol, 5 mM 6-aminocaproic acid, 1 mM EDTA and 1% (v/v) Protease inhibitor cocktail (Sigma). The cells were disrupted with glass beads (0.5 mm diameter) at 5,000 rpm for 20 s using a Mini-bead beater, and this process was repeated three times. Arabidopsis leaves were ground in two-fold buffer(w/v) containing 50 mM imidazole/HCl (pH 7.0), 20% (w/v) glycerol, 5 mM 6-aminocaproic acid, 1 mM EDTA and 1% (v/v) Protease inhibitor cocktail (Sigma). The homogenate was centrifuged at 22,500 × *g* for 1 min at 4 °C. The pellet was washed twice with buffer, resuspended in buffer and mixed with an equivalent volume of 2% (w/v) α-dodecyl maltoside (α-DM) to a final Chl concentration of 0.25–0.5 μg/μL. The 10 μL of Arabidopsis and 10 μL of Chlamydomonas supernatant containing membrane proteins

were separated on a 4–14% acrylamide gradient gel at 4 °C (Takabayashi *et al.*, 2011b). Following electrophoresis, the green bands were excised and heated at 80 °C for 3 min in 100 μL of water. A 100 μL aliquot of sample buffer containing 10% (w/v) sucrose, 125 mM Tris-HCl (pH 6.8), 4% (w/v) SDS, 1% (w/v) bromophenol blue and 10% (v/v) 2-mercaptoethanol was added to the heated sample and equilibrated for 5 min. SDS-PAGE (14% polyacrylamide gel containing 8 M urea) and silver staining were performed as described previously (Takabayashi *et al.*, 2011b).

Low temperature fluorescence analysis. Green bands isolated from BN-PAGE or logarithmic growth phase cells were adjusted to 0.5 μg Chl/mL in 25% (vol/vol) glycerol, placed into glass tubes and frozen in liquid nitrogen. Low temperature emission spectra were measured by exciting frozen samples at 440 nm using a F-2500 fluorescence spectrophotometer (Hitachi).

Immunoblotting analysis. Homogenates were prepared as described for the BN-PAGE and centrifuged at 22,500 × *g* for 1 min at 4 °C. The pellets were washed twice with the same buffer and resuspended in the same volume of sample buffer containing 10% (wt/vol) sucrose, 125 mM Tris-HCl (pH 6.8), 4% (w/v) SDS, 1% (w/v) bromophenol blue and 5% (v/v) 2-mercaptoethanol and heated at 95 °C for 1 min. The homogenate was centrifuged at 22,500 × *g* for 1 min at 4 °C, and the supernatant was resolved using SDS-PAGE. Two-week-old Arabidopsis leaves were homogenized in 20 times (w/v) solubilizing buffer containing 10% (w/v) sucrose, 125 mM Tris-HCl (pH 6.8), 4% (w/v) SDS and 5% (v/v) 2-mercaptoethanol. The homogenate was centrifuged at 22,500 × *g* for 1 min at 4 °C, and 1 μL of supernatant was resolved using SDS-PAGE (14% polyacrylamide gel) and electroblotted to a PVDF membrane. Primary antibodies against CP47 (1:10,000, Agrisera), CP43 (1:10,000) (Tanaka *et al.*, 1991), D1 (1:10,000, Agrisera), D2 (1:10,000, Agrisera), LHCII (1:5,000) (Tanaka *et al.*, 1991), PsaA (1:2,000, Agrisera), PsaC (1:10,000, Agrisera), PsaA/PsaB (1:100,000) (Tanaka *et al.*, 1991) and appropriate secondary antibodies (1:10,000, Sigma) were used.

RNA extraction and qRT-PCR. Total RNA was extracted from Chlamydomonas cells using an RNeasy mini kit (Qiagen), cDNA was synthesized using a PrimeScriptRT reagent kit with gDNA eraser (TaKaRa), and qRT-PCR were performed using an iQ5 Real-time detection system (Bio-Rad). The primer pairs are listed in Table.S3 and Chlamydomonas G protein β-subunit-like polypeptide (CBLP) was used as a control. The data were analyzed using iQ5 Optical system software (Bio-Rad).

Chlorophyll/P700 measurement. Chlamydomonas cells were collected at the logarithmic growth phase using centrifugation at 7,000 × *g* for 5 min at 4 °C, and resuspended in buffer containing 25mM Tricine-NaOH (pH 8.0), and 0.1% Nonidet P-40 by adjusting the chlorophyll content at

20μg/mL as previously described. (Tanaka *et al.*, 1991)

Dark treatment of the Arabidopsis-complemented line. Arabidopsis was grown on soil at 22 °C under long day (16h cool-white fluorescent light (90-100 μmol photons m^{-2} s^{-1})/8 h dark) conditions. The detached leaves were transferred to a whole set of tissue culture plates (24 well) with water in the holes at the outermost side of the plate. The plates were sealed and covered with aluminum foil.

Acknowledgements

We thank Ryouichi Tanaka and Atsushi Takabayashi for their useful technical suggestions. This work was supported by JSPS KAKENHI Grants-in-Aid for Scientific Research B 15H04381 (A.T.) and Scientific Research C 17K07430 (H.I.), Y.C. was supported by the Ministry of Education, Culture, Sports, Science and Technology of Japan and by the China Scholarship Council.

Conflict of Interest Statement

No conflict.

Short supporting legends

Fig. S1. Genomic PCR confirmation of the null Chlamydomonas sgr mutant.

Fig. S2. Growth rates under photomixotrophic and photoautotrophic conditions.

Fig. S3. Low temperature fluorescence spectra of the green bands resolved by BN-PAGE.

Fig. S4. Silver staining of the photosystems of Chlamydomonas sgr mutant.

Fig. S5. Low temperature fluorescence spectra of the Chlamydomonas cells.

Fig. S6. Chlorophyll degradation under nitrogen starvation in photoautotrophic conditions.

Fig. S7. Complementation of the Arabidopsis sgr triple mutant phenotype by CrSGR.

Fig. S8. Pheo a/Chl ratios of the WT and PsbD mutant during growth phase.

REFERENCES

Armstead, I., Donnison, I., Aubry, S., Harper, J., Hortensteiner, S., James, C., Mani, J., Moffet, M., Ougham, H., Roberts, L., Thomas, A., Weeden, N., Thomas, H. and King, I. (2007) Cross-species identification of Mendel's I locus. *Science*, **315**, 73.

Barry, C.S., McQuinn, R.P., Chung, M.Y., Besuden, A. and Giovannoni, J.J. (2008) Amino acid substitutions in homologs of the STAY-GREEN protein are responsible for the green-flesh and chlorophyll retainer mutations of tomato and pepper. *Plant Physiol.*, **147**, 179-187.

Bell, A., Moreau, C., Chinoy, C., Spanner, R., Dalmais, M., Le Signor, C., Bendahmane, A., Klenell, M. and Domoney, C. (2015) SGRL can regulate chlorophyll metabolism and contributes to normal plant growth and development in Pisum sativum L. *Plant Mol. Biol.*, **89**, 539-558.

Cha, K.W., Lee, Y.J., Koh, H.J., Lee, B.M., Nam, Y.W. and Paek, N.C. (2002) Isolation, characterization, and mapping of the stay green mutant in rice. *Theor. Appl. Genet.*, **104**, 526-532.

Chidgey, J.W., Linhartova, M., Komenda, J., Jackson, P.J., Dickman, M.J., Canniffe, D.P., Konik, P., Pilny, J., Hunter, C.N. and Sobotka, R. (2014) A cyanobacterial chlorophyll synthase-HliD complex associates with the Ycf39 protein and the YidC/Alb3 insertase. *Plant Cell*, **26**, 1267-1279.

Christ, B. and Hortensteiner, S. (2014) Mechanism and Significance of Chlorophyll Breakdown. *J. Plant Growth Regul.*, **33**, 4-20.

Drop, B., Webber-Birungi, M., Yadav, S.K.N., Filipowicz-Szymanska, A., Fusetti, F., Boekema, E.J. and Croce, R. (2014) Light-harvesting complex II (LHCII) and its supramolecular organization in Chlamydomonas reinhardtii. *Biochim Biophys Acta*, **1837**, 63-72.

Erickson, J.M., Rahire, M., Malnoe, P., Girard-Bascou, J., Pierre, Y., Bennoun, P. and Rochaix, J.D. (1986) Lack of the D2 protein in a Chlamydomonas reinhardtii psbD mutant affects photosystem II stability and D1 expression. *EMBO J.*, **5**, 1745-1754.

Guenther, J.E., Nemson, J.A. and Melis, A. (1990) Development of photosystem-II in dark-grown Chlamydomonas-reinhardtii. A light-dependent conversion of PSIIα, Qb-nonreducing centers to the PS IIα, Qb-reducing form. *Photosynthesis Res.*, **24**, 35-46.

Hortensteiner, S. (2006) Chlorophyll degradation during senescence. *Annu. Rev. Plant Biol.*, **57**, 55-77.

Hortensteiner, S. (2013) Update on the biochemistry of chlorophyll breakdown. *Plant Mol. Biol.*, **82**, 505-517.

Jiang, H., Li, M., Liang, N., Yan, H., Wei, Y., Xu, X., Liu, J., Xu, Z., Chen, F. and Wu, G. (2007) Molecular cloning and function analysis of the stay green gene in rice. *Plant J.*, **52**, 197-209.

Komenda, J., Sobotka, R. and Nixon, P.J. (2012) Assembling and maintaining the Photosystem II complex in chloroplasts and cyanobacteria. *Curr. Opin. Plant Biol.*, **15**, 245-251.

Kunugi, M., Satoh, S., Ihara, K., Shibata, K., Yamagishi, Y., Kogame, K., Obokata, J., Takabayashi, A. and Tanaka, A. (2016) Evolution of green plants accompanied changes in light-harvesting systems. *Plant Cell Physiol.*, **57**, 1231-1243.

Leliaert, F., Verbruggen, H. and Zechman, F.W. (2011) Into the deep: New discoveries at the base of the green plant phylogeny. *BioEssays*, **33**, 683-692.

Maroc, J. and Tremolieres, A. (1990) Chlorophyll-a' and pheophytin-a, as determined by HPLC, in photosynthesis mutants and double mutants of chlamydomonas-Reinhardtii. *Biochim. Biophys. Acta*, **1018**, 67-71.

Matsuda, K., Shimoda, Y., Tanaka, A. and Ito, H. (2016) Chlorophyll a is a favorable substrate for Chlamydomonas Mg-dechelatase encoded by STAY-GREEN. *Plant Physiol. Biochem.*, **109**, 365-373.

Matsuo, T., Okamoto, K., Onai, K., Niwa, Y., Shimogawara, K. and Ishiura, M. (2008) A systematic forward genetic analysis identified components of the Chlamydomonas circadian system. *Genes Dev.*, **22**, 918-930.

Nelson, N. and Junge, W. (2015) Structure and Energy Transfer in Photosystems of Oxygenic Photosynthesis. *Annu Rev Biochem*, **84**, 659-683.

Nickelsen, J. and Rengstl, B. (2013) Photosystem II Assembly: From Cyanobacteria to Plants. *Annu Rev Plant Biol*, **64**, 609-635.

Nosek, L., Semchonok, D., Boekema, E.J., Ilik, P. and Kouril, R. (2017) Structural variability of plant photosystem II megacomplexes in thylakoid membranes. *Plant J.*, **89**, 104-111.

Park, S.Y., Yu, J.W., Park, J.S., Li, J., Yoo, S.C., Lee, N.Y., Lee, S.K., Jeong, S.W., Seo, H.S., Koh, H.J., Jeon, J.S., Park, Y.I. and Paek, N.C. (2007) The senescence-induced staygreen protein regulates chlorophyll degradation. *Plant Cell*, **19**, 1649-1664.

Pilkington, S.M., Montefiori, M., Jameson, P.E. and Allan, A.C. (2012) The control of chlorophyll levels in maturing kiwifruit. *Planta*, **236**, 1615-1628.

Plochinger, M., Schwenkert, S., von Sydow, L., Schroder, W.P. and Meurer, J. (2016) Functional update of the auxiliary proteins PsbW, PsbY, HCF136,PsbN, TerC and ALB3 in Maintenance and assembly of PSII. *Front Plant Sci*, **7**.

Pruzinska, A., Tanner, G., Anders, I., Roca, M. and Hortensteiner, S. (2003) Chlorophyll

breakdown: pheophorbide a oxygenase is a Rieske-type iron-sulfur protein, encoded by the accelerated cell death 1 gene. *Proc Natl Acad Sci U S A*, **100**, 15259-15264.

Qian, L.W., Voss-Fels, K., Cui, Y.X., Jan, H.U., Samans, B., Obermeier, C., Qian, W. and Snowdon, R.J. (2016) Deletion of a stay-green gene associates with adaptive selection in brassica napus. *Mol Plant*, **9**, 1559-1569.

Ren, G.D., An, K., Liao, Y., Zhou, X., Cao, Y.J., Zhao, H.F., Ge, X.C. and Kuai, B.K. (2007) Identification of a novel chloroplast protein AtNYE1 regulating chlorophyll degradation during leaf senescence in arabidopsis. *Plant Physiol.*, **144**, 1429-1441.

Rengstl, B., Oster, U., Stengel, A. and Nickelsen, J. (2011) An intermediate membrane subfraction in cyanobacteria is involved in an assembly network for photosystem II Biogenesis. *J. Biol. Chem.*, **286**, 21944-21951.

Rong, H., Tang, Y.Y., Zhang, H., Wu, P.Z., Chen, Y.P., Li, M.R., Wu, G.J. and Jiang, H.W. (2013) The Stay-Green Rice like (SGRL) gene regulates chlorophyll degradation in rice. *J. Plant Physiol.*, **170**, 1367-1373.

Saga, Y., Hirai, Y., Sadaoka, K., Isaji, M. and Tamiaki, H. (2013) Structure-dependent demetalation kinetics of chlorophyll a analogs under acidic conditions. *Photochem. Photobiol.*, **89**, 68-73.

Sakuraba, Y., Balazadeh, S., Tanaka, R., Mueller-Roeber, B. and Tanaka, A. (2012a) Overproduction of Chl b Retards Senescence Through Transcriptional Reprogramming in Arabidopsis. *P Plant Cell Physiol*, **53**, 505-517.

Sakuraba, Y., Park, S.Y. and Paek, N.C. (2015) The divergent roles of STAYGREEN (SGR) homologs in chlorophyll degradation. *Mol Cells*, **38**, 390-395.

Sakuraba, Y., Schelbert, S., Park, S.Y., Han, S.H., Lee, B.D., Andres, C.B., Kessler, F., Hortensteiner, S. and Paek, N.C. (2012b) STAY-GREEN and chlorophyll catabolic enzymes interact at light-harvesting complex II for chlorophyll detoxification during leaf senescence in Arabidopsis. *Plant Cell*, **24**, 507-518.

Schelbert, S., Aubry, S., Burla, B., Agne, B., Kessler, F., Krupinska, K. and Hortensteiner, S. (2009) Pheophytin pheophorbide hydrolase (pheophytinase) is involved in chlorophyll breakdown during leaf senescence in Arabidopsis. *Plant Cell*, **21**, 767-785.

Schmollinger, S., Muhlhaus, T., Boyle, N.R., Blaby, I.K., Casero, D., Mettler, T., Moseley, J.L., Kropat, J., Sommer, F., Strenkert, D., Hemme, D., Pellegrini, M., Grossman, A.R., Stitt, M., Schroda, M. and Merchant, S.S. (2014) Nitrogen-sparing mechanisms in Chlamydomonas affect the transcriptome, the proteome, and photosynthetic metabolism. *Plant Cell*, **26**, 1410-1435.

Schulz-Raffelt, M., Chochois, V., Auroy, P., Cuine, S., Billon, E., Dauvillee, D., Li-Beisson, Y.

and Peltier, G. (2016) Hyper-accumulation of starch and oil in a Chlamydomonas mutant affected in a plant-specific DYRK kinase. *Biotechnol Biofuels*, **9**, 55.

Sharma, S.K., Nelson, D.R., Abdrabu, R., Khraiwesh, B., Jijakli, K., Arnoux, M., O'Connor, M.J., Bahmani, T., Cai, H., Khapli, S., Jagannathan, R. and Salehi-Ashtiani, K. (2015) An integrative Raman microscopy-based workflow for rapid in situ analysis of microalgal lipid bodies. *Biotechnol Biofuels*, **8**.

Shimoda, Y., Ito, H. and Tanaka, A. (2016) Arabidopsis STAY-GREEN, Mendel's green cotyledon gene, Encodes magnesium-dechelatase. *Plant Cell*, **28**, 2147-2160.

Sirpio, S., Khrouchtchova, A., Allahverdiyeva, Y., Hansson, M., Fristedt, R., Vener, A.V., Scheller, H.V., Jensen, P.E., Haldrup, A. and Aro, E.M. (2008) AtCYP38 ensures early biogenesis, correct assembly and sustenance of photosystem II. *Plant J.*, **55**, 639-651.

Takabayashi, A., Kurihara, K., Kuwano, M., Kasahara, Y., Tanaka, R. and Tanaka, A. (2011a) The oligomeric states of the photosystems and the light-harvesting complexes in the Chl b-less mutant. *Plant Cell Physiol.*, **52**, 2103-2114.

Takabayashi, A., Kurihara, K., Kuwano, M., Kasahara, Y., Tanaka, R. and Tanaka, A. (2011b) The Oligomeric States of the Photosystems and the Light-Harvesting Complexes in the Chl b-Less Mutant. *Plant Cell Physiol.*, **52**, 2103-2114.

Tanaka, A., Ito, H., Tanaka, R., Tanaka, N.K., Yoshida, K. and Okada, K. (1998) Chlorophyll a oxygenase (CAO) is involved in chlorophyll b formation from chlorophyll a. *Proc Natl Acad Sci U S A*, **95**, 12719-12723.

Tanaka, A., Yamamoto, Y. and Tsuji, H. (1991) Formation of chlorophyll-protein complexes during greening 2. Redistribution of chlorophyll among apoproteins. *Plant Cell Physiol.*, **32**, 195-204.

Theis, J. and Schroda, M. (2016) Revisiting the photosystem II repair cycle. *Plant Signaling & Behavior*, **11**.

Umena, Y., Kawakami, K., Shen, J.R. and Kamiya, N. (2011) Crystal structure of oxygen-evolving photosystem II at a resolution of 1.9 angstrom. *Nature*, **473**, 55-U65.

Uniacke, J. and Zerges, W. (2007) Photosystem II assembly and repair are differentially localized in Chlamydomonas. *Plant Cell*, **19**, 3640-3654.

Wu, S.X., Li, Z.P., Yang, L.F., Xie, Z.K., Chen, J.Y., Zhang, W., Liu, T.Q., Gao, S., Gao, J., Zhu, Y.H., Xin, J.W., Ren, G.D. and Kuai, B.K. (2016) NON-YELLOWING2 (NYE2), a close paralog of NYE1, plays a positive role in chlorophyll degradation in Arabidopsis. *Mol Plant*, **9**, 624-627.

Yokono, M., Takabayashi, A., Akimoto, S. and Tanaka, A. (2015) A megacomplex composed of

both photosystem reaction centres in higher plants. *Nature Communications*, **6**.

Zhang, S.L., Frankel, L.K. and Bricker, T.M. (2010) The Sll0606 protein Is required for photosystem II assembly/stability in the cyanobacterium Synechocystis sp. PCC 6803. *J. Biol. Chem.*, **285**, 32047-32054.

Zhou, C.E., Han, L., Pislariu, C., Nakashima, J., Fu, C.X., Jiang, Q.Z., Quan, L., Blancaflor, E.B., Tang, Y.H., Bouton, J.H., Udvardi, M., Xia, G.M. and Wang, Z.Y. (2011) From model to crop: Functional analysis of a STAY-GREEN gene in the Model legume Medicago truncatula and effective use of the gene for Alfalfa Improvement. *Plant Physiol.*, **157**, 1483-1496.

Figure Legends

Fig. 1. Effect of light intensity on Fv/Fm ratios. (*A*) Stationary growth phase Chlamydomonas cells exposed to low light (1 μmol photons m^{-2} s^{-1}, LL1), normal light (80 μmol photons m^{-2} s^{-1}, NL80), or high light (250 μmol photons m^{-2} s^{-1}, HL250) for 2 d. (*B*) Stationary growth phase cells exposed to strong light (750 μmol photons m^{-2} s^{-1}). The Fv/Fm ratios were measured after 10 min of dark acclimation. Measurements from 3–6 biological replicates (mean ± SD) that were significantly different from WT are indicated (****** $P < 0.01$, ***** $P < 0.05$, Student's *t* test).

Fig. 2. Pheo *a*/Chl ratios during the growth phase. Chlamydomonas cells were grown in TAP media at 80 μmol photons m^{-2} s^{-1} and were inoculated at an optical density of 0.1 at 750 nm. Measurements from 3–6 biological replicates (mean ± SD) that were significantly different from the WT are indicated (****** $P < 0.01$, ***** $P < 0.05$, Student's *t* test).

Fig. 3. BN-PAGE analysis and silver staining of the photosystems of Chlamydomonas. (*A*) Chlamydomonas cells were grown in TAP media at 80 μmol photons m^{-2} s^{-1} to the logarithmic growth phase, and the photosystems were resolved using BN-PAGE. (*B*) Green bands from the WT cells were resolved by BN-PAGE and were excised and examined using SDS-PAGE and silver staining.

Fig. 4. Immunoblotting analysis of photosynthetic proteins of Chlamydomonas. Chlamydomonas cells were grown in TAP media at 80 μmol photons m^{-2} s^{-1} (NL80). Membrane proteins isolated from logarithmic growth phase cells, corresponding to 0.2 μg Chl (CP47, CP43, D1, PsaA and PsaC) or 0.1 μg Chl (D2 and LHCII), were analyzed by immunoblotting. Dilution series (1, 1/2 and 1/4) were prepared to compare the protein levels.

Fig. 5. Chl degradation and gene expression with nitrogen starvation. Chlamydomonas cells were grown in TAP medium at 80 μmol photons m^{-2} s^{-1} and transferred to TAP or nitrogen-depleted media. (*A*) Pictures of cultures during nitrogen starvation. (*B*) Changes in the Chl content during nitrogen starvation. Measurements from 3–6 biological replicates (mean ± SD) that were significantly different between day 7 and day 0 are indicated (****** $P < 0.01$, ***** $P < 0.05$, Student's *t* test). (*C*) Relative mRNA expression levels of SGR, NYC1 (NON-YELLOW COLORING1) and PaO (Pheophorbide *a* oxygenase) at day 3 of nitrogen starvation. Measurements from 3–6 biological replicates (mean ± SD) that were significantly different between TAP-N- and TAP-N+ are indicated (****** $P < 0.01$, Student's *t* test). # PaO is closely related to a vascular plant PaOs, but it has not yet been enzymatically identified.

Fig. 6. Phenotypes of Arabidopsis *sgr* mutants. (*A*) Photograph of 3-week-old plants. (*B*) Immunoblotting analysis of photosynthetic proteins isolated from developing leaves. (*C*) Fv/Fm ratios of leaves from 3-week-old plants grown at 80 μmol photons m^{-2} s^{-1} were measured after 10 min of dark acclimation. Measurements from 3 biological replicates (mean ± SD) that were significantly different from the WT are indicated (****** $P < 0.01$, Student's *t* test). (*D*) Photograph of natural senescence stage plants. (*E*) BN-PAGE analysis before and after 6 days of dark-incubation.

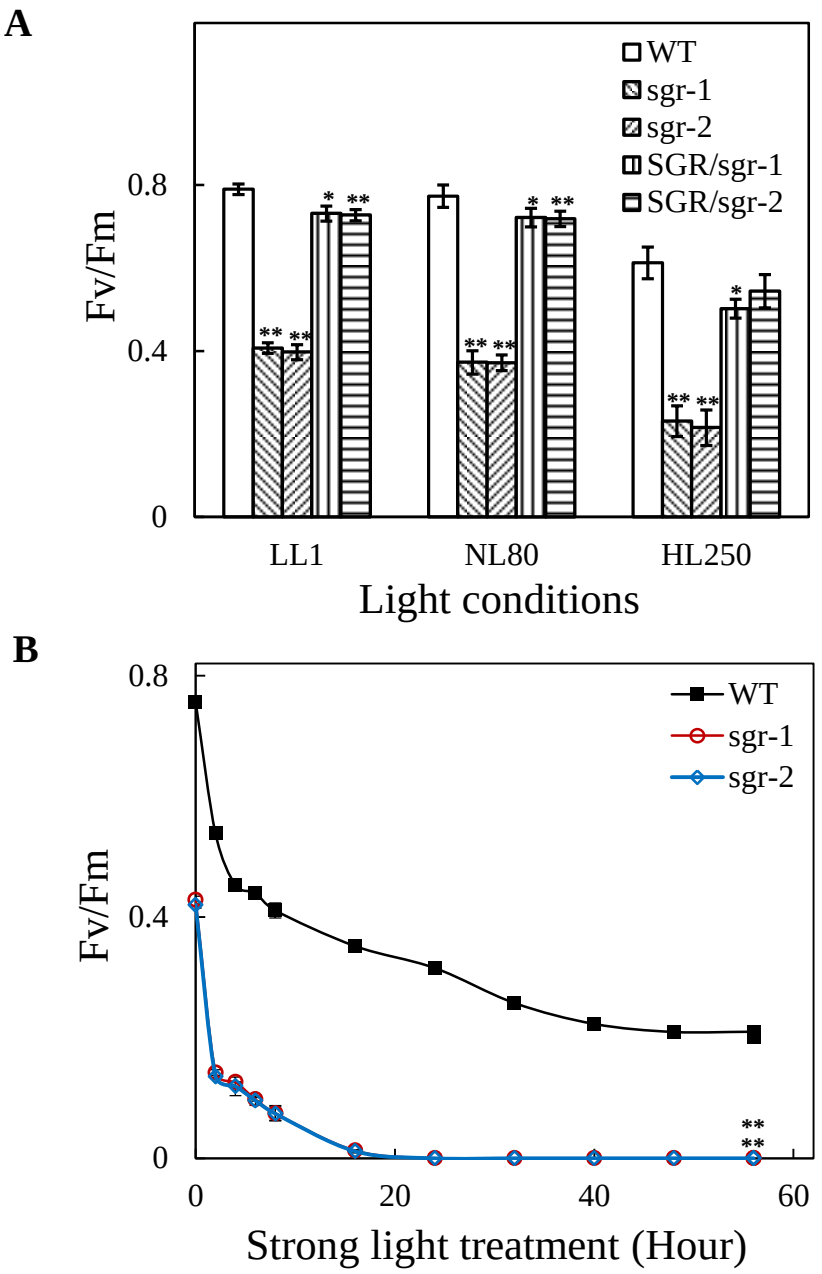
A
WT
sgr-1
sgr-2
SGR/sgr-1
SGR/sgr-2
Fv/Fm
0.8
0.4
0
LL1
NL80
HL250
Light conditions
B
WT
sgr-1
sgr-2
Fv/Fm
0.8
0.4
0
0
20
40
60
Strong light treatment (Hour)

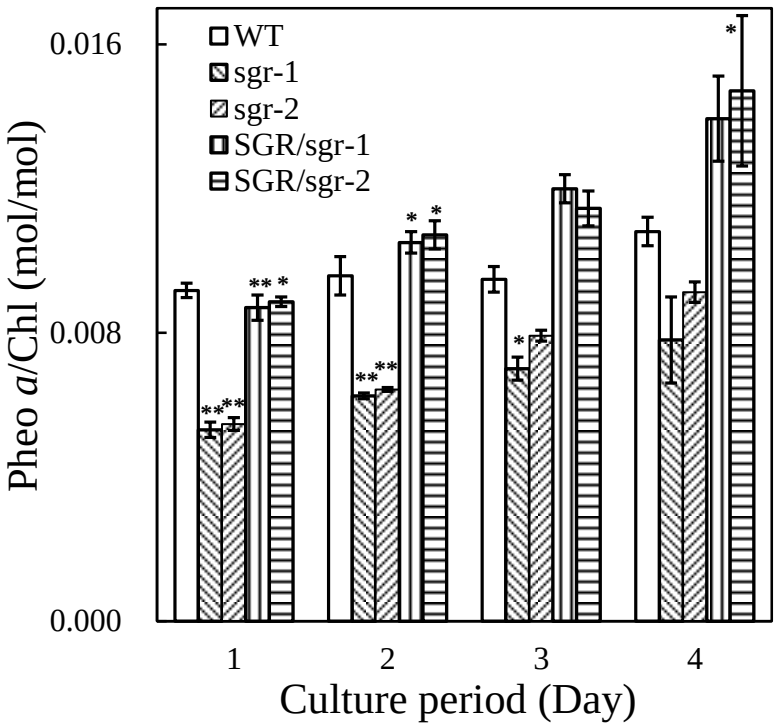
WT
sgr-1
sgr-2
SGR/sgr-1
SGR/sgr-2
0.016
0.008
0.000
Pheo a/Chl (mol/mol)
1
2
3
4
Culture period (Day)

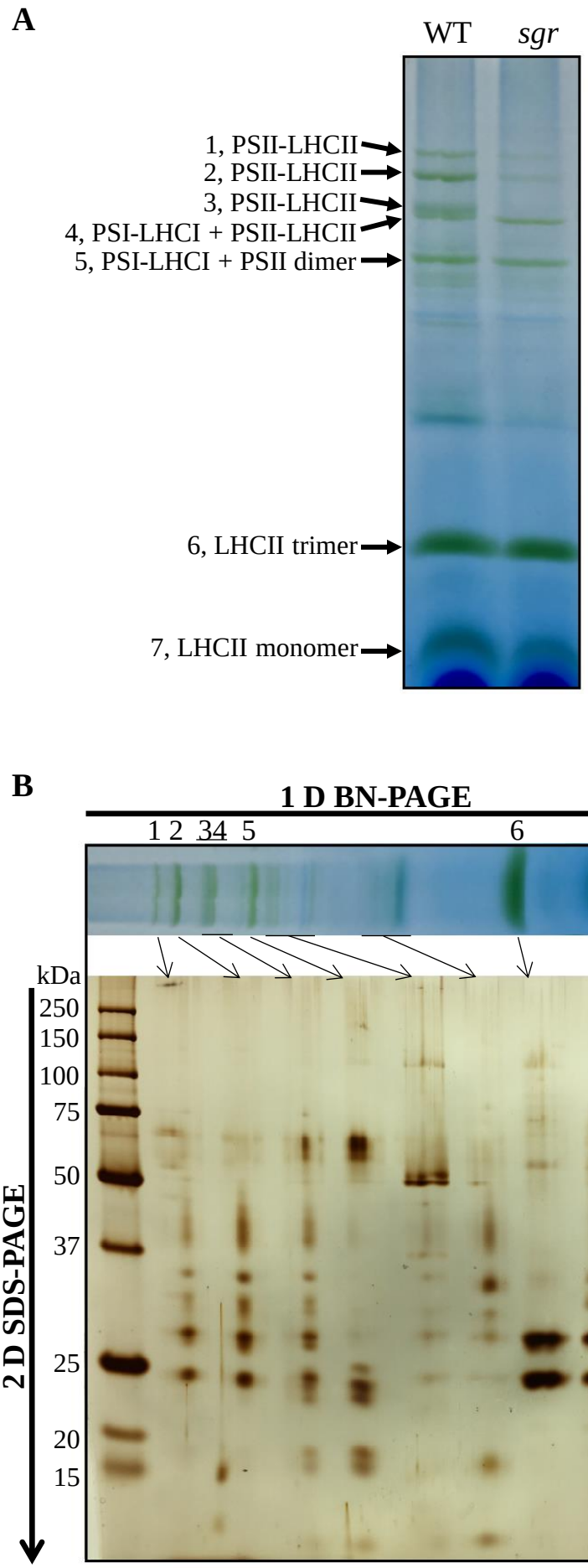
A
WT
sgr
1, PSII-LHCII
2, PSII-LHCII
3, PSII-LHCII
4, PSI-LHCI + PSII-LHCII
5, PSI-LHCI + PSII dimer
6, LHCII trimer
7, LHCII monomer
B
1 D BN-PAGE
1 2 34 5
6
7
kDa
250
150
100
75
50
37
25
20
15
2 D SDS-PAGE

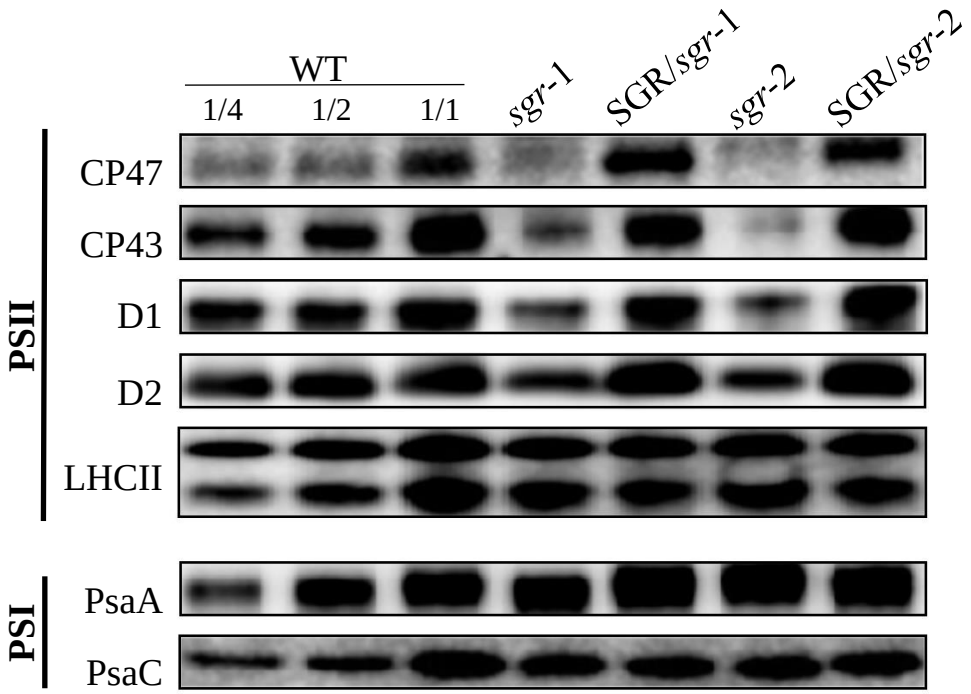
WT
1/4
1/2
1/1
sgr-1
SGR/sgr-1
sgr-2
SGR/sgr-2
PSII
CP47
CP43
D1
D2
LHCII
PSI
PsaA
PsaC

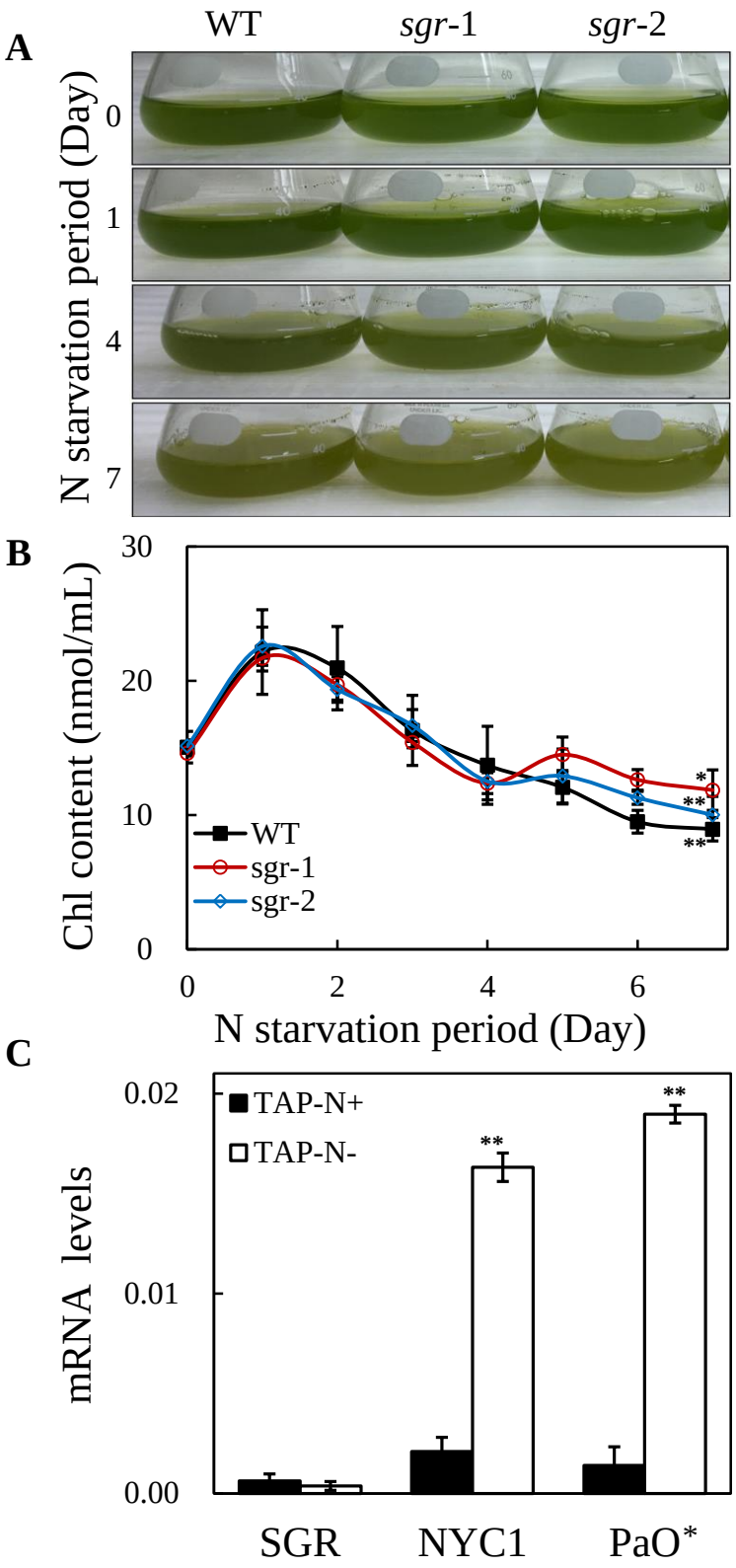
A
WT
sgr-1
sgr-2
N starvation period (Day)
0
1
4
7
B
Chl content (nmol/mL)
30
20
10
0
0
2
4
6
N starvation period (Day)
WT
sgr-1
sgr-2
*
**
**
C
mRNA levels
0.02
0.01
0.00
TAP-N+
TAP-N-
**
**
SGR
NYC1
PaO*

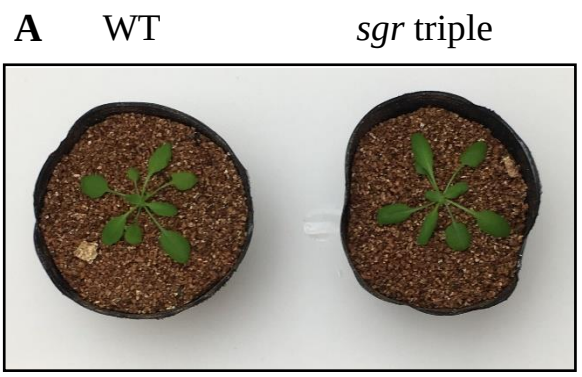
A
WT
sgr triple

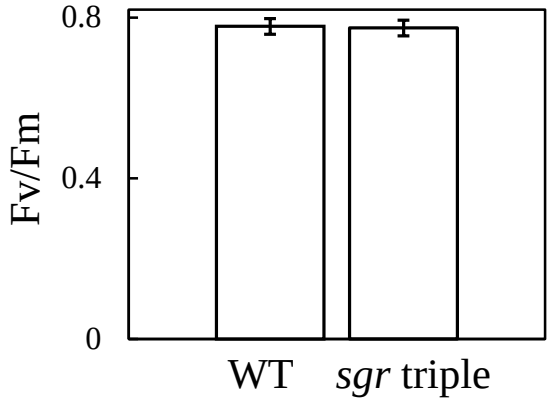
C
0.8
0.4
0
Fv/Fm
WT
sgr triple

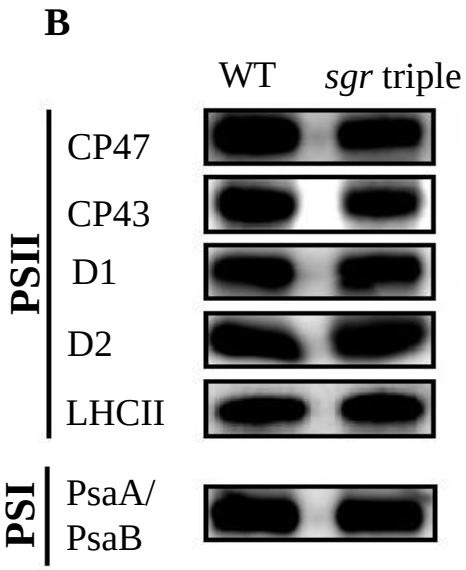
B
WT
sgr triple
PSII
CP47
CP43
D1
D2
LHCII
PSI
PsaA/
PsaB


D
WT
sgr triple

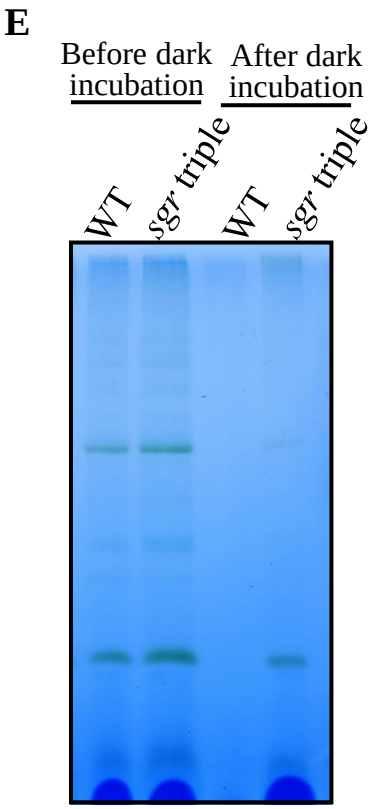
E
Before dark incubation
After dark incubation
WT
sgr triple
WT
sgr triple

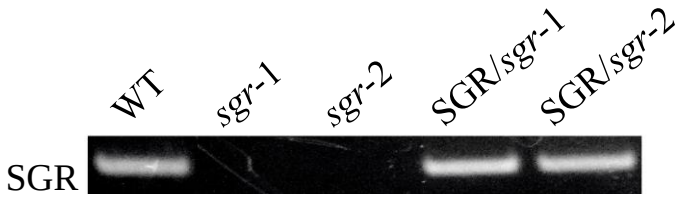

Fig. S1. Genomic PCR confirmation of the null Chlamydomonas *sgr* mutant. Chlamydomonas cells were grown in TAP media at 80 μmol photons m^{-2} s^{-1}.

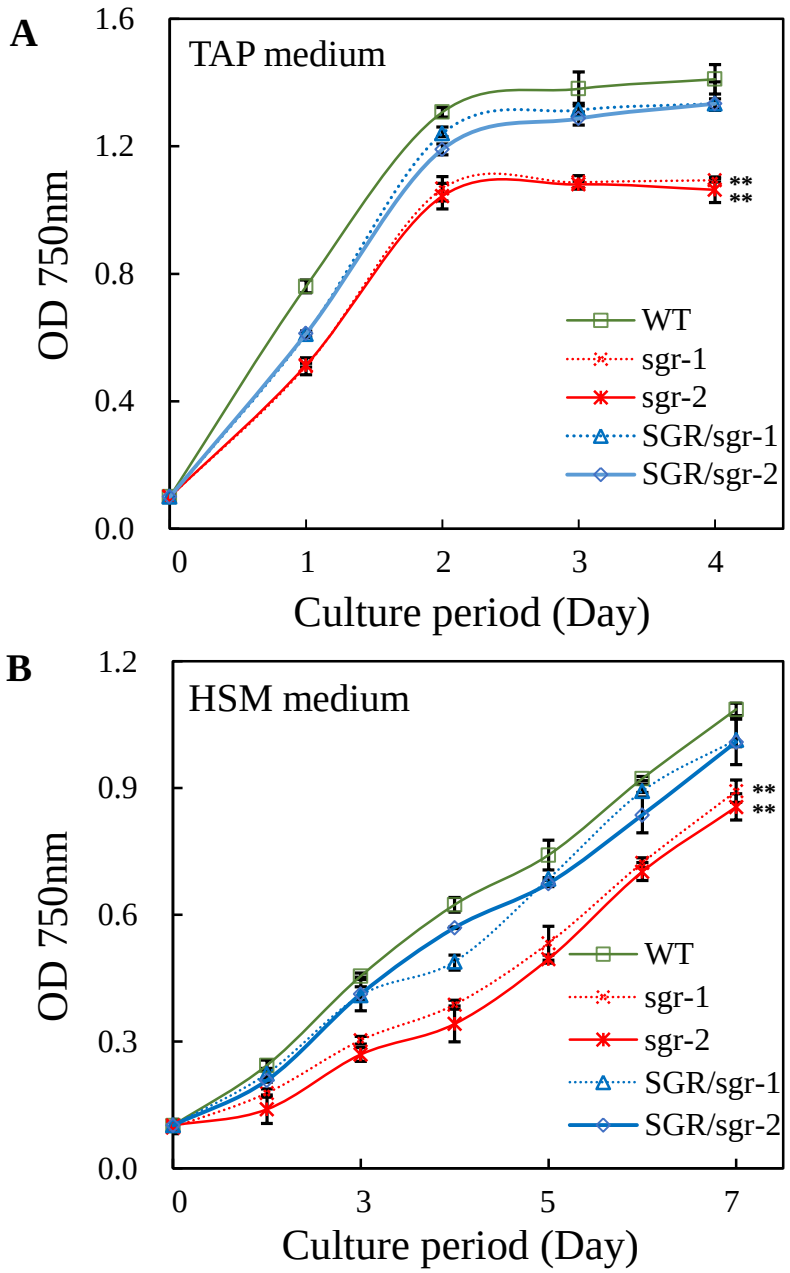

Fig. S2. Growth rates under photomixotrophic and photoautotrophic conditions. Chlamydomonas cells grown at 80 µmol photons m^{-2} s^{-1} were inoculated at an optical density of 0.1 at 750 nm and grown photomixotrophically on TAP media (*A*) or photoautotrophically on HSM media (*B*). Measurements from 3–6 biological replicates (mean ± SD) that were significantly different from the WT are indicated (****** $P < 0.01$, Student's *t* test).

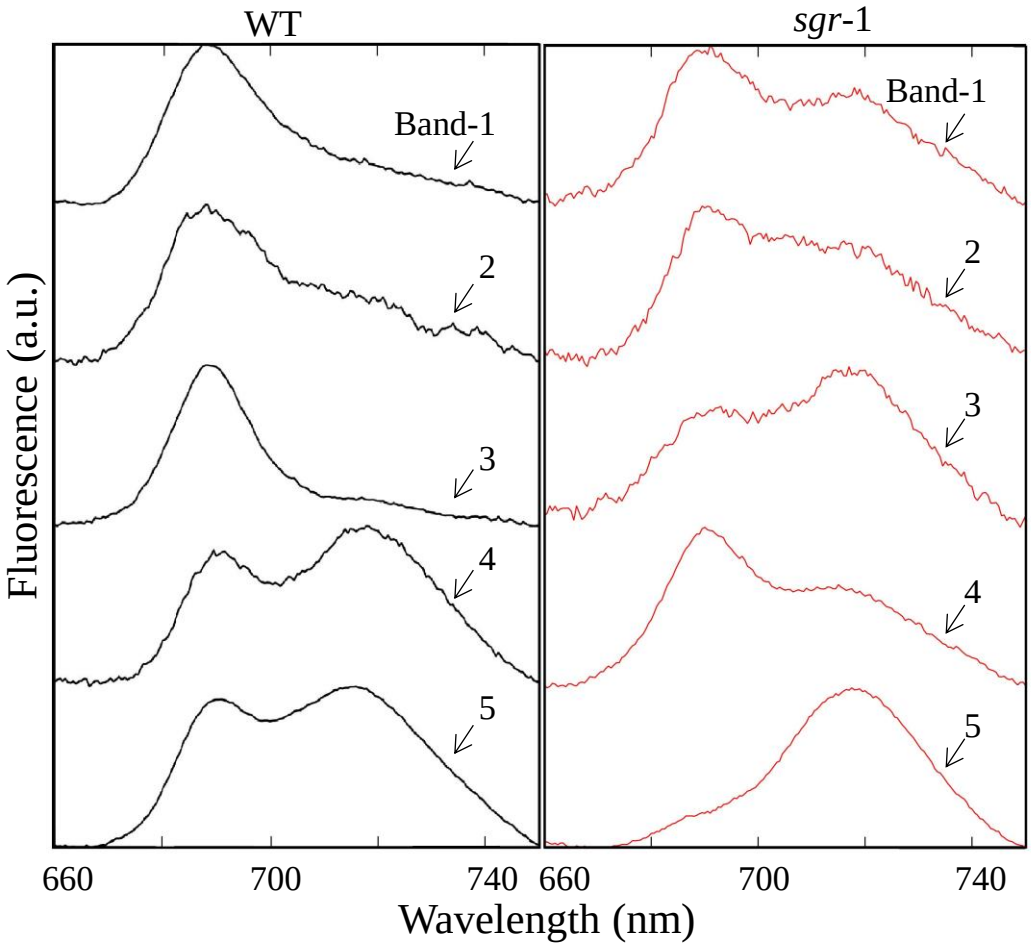

Fig. S3. Low temperature fluorescence spectra of the green bands resolved by BN-PAGE. Green bands 1 to 5 from the WT and the Chlamydomonas *sgr* mutant were excised, and the fluorescence emission spectra at 440 nm excitation were directly measured in liquid nitrogen. For each green band, the means of 60 spectra are presented.

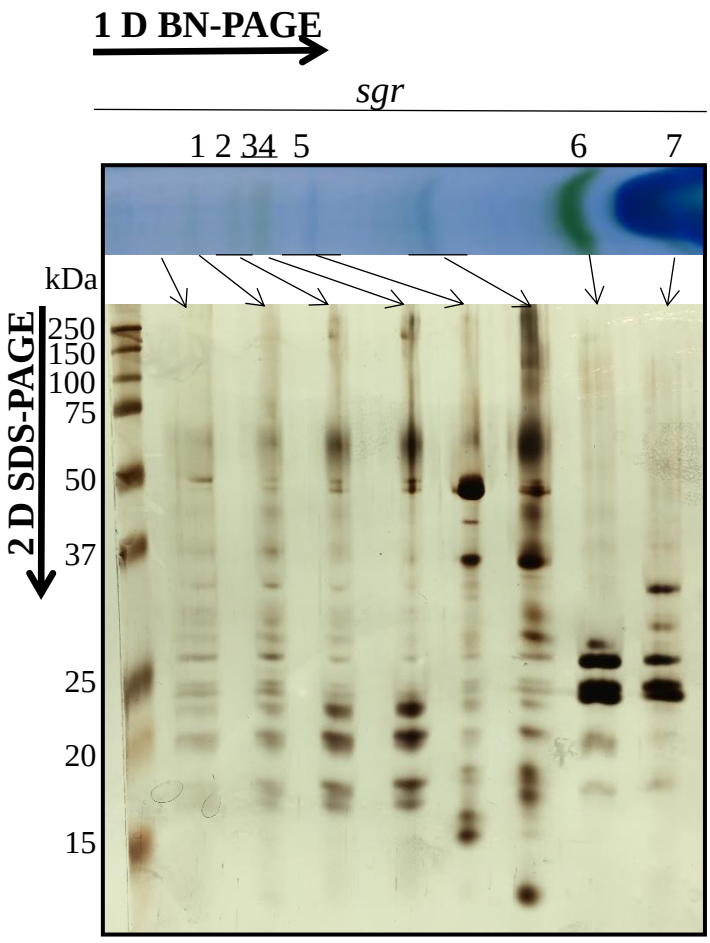

Fig. S4. Silver staining of the photosystems of Chlamydomonas *sgr* mutant. Chlamydomonas *sgr* mutant cells were grown in TAP media at 80 μmol photons m^{-2} s^{-1} to the logarithmic growth phase, and the photosystems were resolved using BN-PAGE. Bands from the *sgr* cells were excised and examined using SDS-PAGE and silver staining.

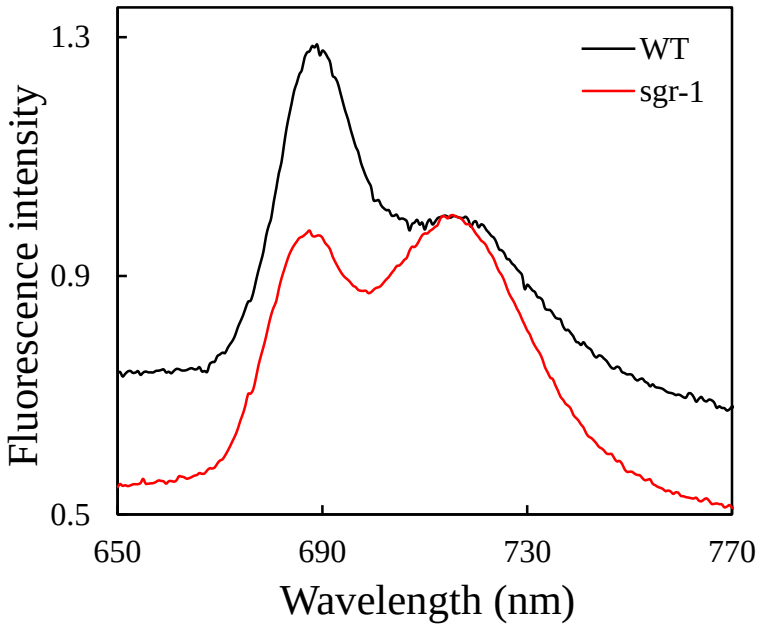

Fig. S5. Low temperature fluorescence spectra of the Chlamydomonas cells. Chlamydomonas cells grown at 80 μmol photons m^{-2} s^{-1} were harvested at early logarithmic growth phase, and the fluorescence emission spectra at 440 nm excitation were directly measured in liquid nitrogen. The fluorescence spectra were normalized at 710 nm, and the means of 20 spectra are presented.

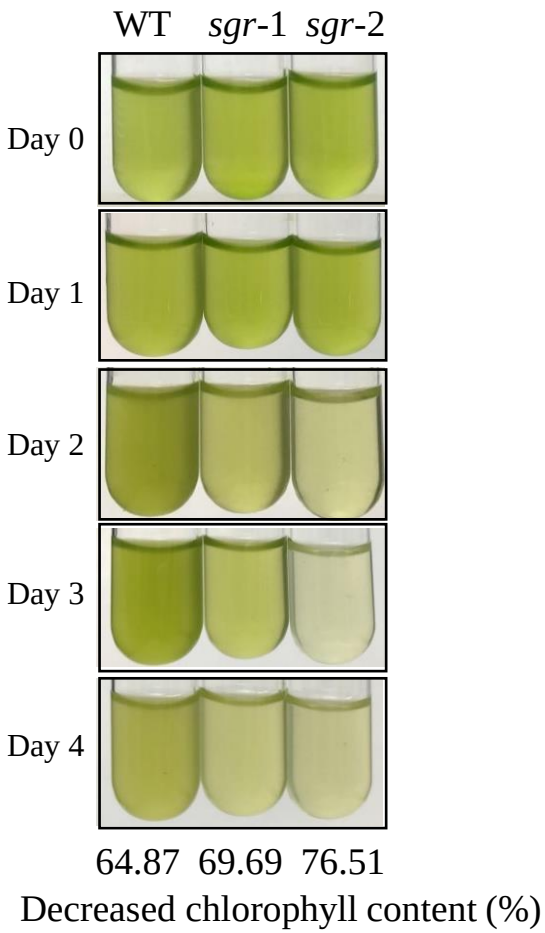

Fig. S6. Chlorophyll degradation under nitrogen starvation in photoautotrophic conditions. Chlamydomonas cells were grown in TAP media at 80 μmol photons m^{-2} s^{-1} and were transferred to N depleted TP media with 5% CO_2 continuous positive airway pressure.

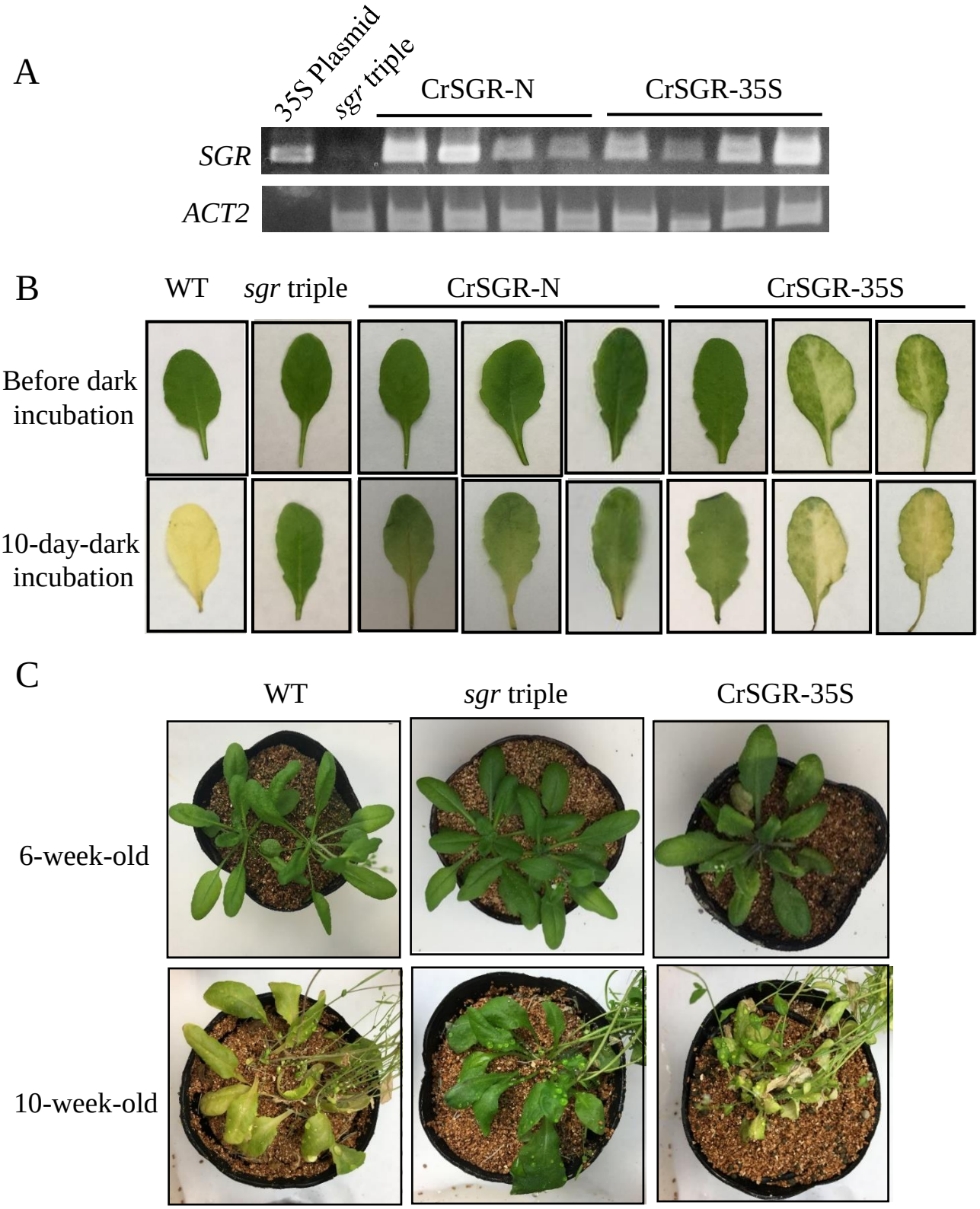

Fig. S7. Complementation of the Arabidopsis *sgr* triple mutant phenotype by CrSGR. (*A*) Genomic PCR confirmation of the complemented Arabidopsis lines. 35S Plasmid for Arabidopsis complementation is used as positive control, and *ACT2* is used as control. (*B*) The picture of dark-induced senescent leaves. Three-week-old Arabidopsis detached leaves were incubated in the dark for 10 days. (*C*) The picture of natural senescent plants.

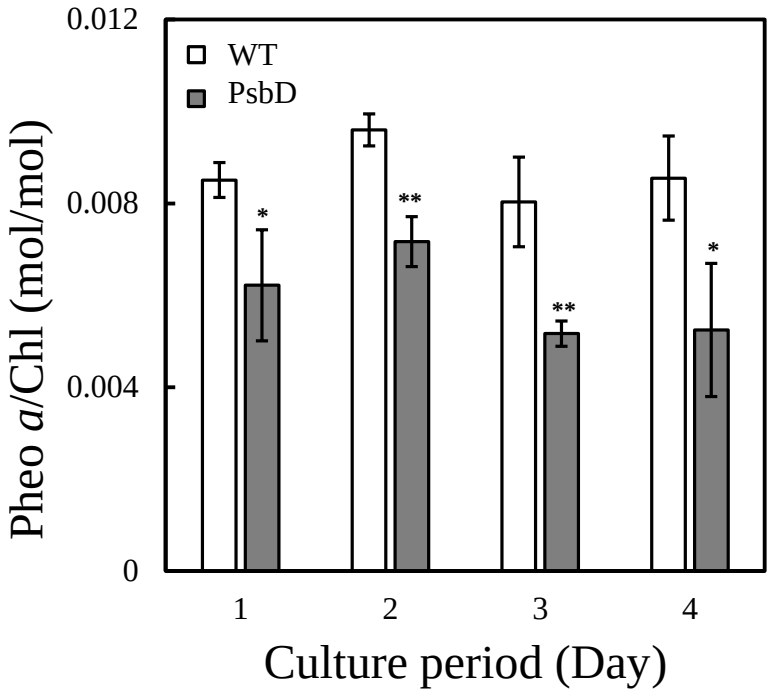

Fig. S8. Pheo *a*/Chl ratios of the WT and PsbD mutant during growth phase. Chlamydomonas cells were grown in TAP media at 80 μmol photons m^{-2} s^{-1} and were inoculated at an optical density of 0.1 at 750 nm. Measurements from 3–6 biological replicates (mean ± SD) that were significantly different from the WT are indicated (****** $P < 0.01$, ***** $P < 0.05$, Student's *t* test).

Table. S1. Chlorophyll/P700 ratio in Chlamydomonas.

	WT	*sgr*-2
Chl/P700	310±38	240±35

Table. S2. Pigment content of Arabidopsis WT and *sgr* triple mutant.

Name		Chl *a* (nmol cm^{-2})	Chl *b* (nmol cm^{-2})	Pheo *a* (nmol cm^{-2})	Neo (HPLC area cm^{-2})	Viol (HPLC area cm^{-2})
Before dark incubation	WT	27.79±10.90	8.89±3.26	12.40±5.40	3654.60±1371.97	3077.30±1226.87
	sgr triple	32.48±5.71	9.51±1.73	12.40±5.40	3797.28±494.12	1398.36±615.61
After dark incubation	WT	2.82±0.65	0.78±0.17	12.40±5.40	399.92±88.97	898.81±169.15
	sgr triple	16.26±4.55	2.71±1.25	18.08±5.48	2240.54±573.01	1832.53±715.19

Table. S3. Primer list of qRT-PCR for nitrogen starvation and PCR for preparation and confirmation of Arabidopsis and Chlamydomonas complimented lines.

Name	Primer sequence (5’ to 3’)	Experiments
NYC1-F	CGGGTGGAGGACACATCTTC	qRT-PCR
NYC1-R	TGACTGTGTGCAGCTTGATG	qRT-PCR
PaO-F	CAAGCTCATCTCGAACATCC	qRT-PCR
PaO-R	GCCACTCATCTCGAACATCC	qRT-PCR
SGR-F	TTCATTTCCAGTCCAGCGTG	qRT-PCR
SGR-R	CGATGATGGCGTAAATGGTG	qRT-PCR
CBLP-F	GATGTGCTGTCCGTGGCTTTC	qRT-PCR
CBLP-R	ACGATGATGGGGTTGGTGGTC	qRT-PCR
Cr_SGR-F	CACTCAACATCTTACGGTAAGTA TGTTAGACACGACTTGG	Chlamydomonas complementation
Cr_SGR-R	TCATATGGCGGCCGCCAACAGGT CATGTTACAGGGGGCAT	Chlamydomonas complementation
AtSGR1_promoter-F	GCAGGCTCCACCATGGATTGCAG GATGTTATAAG	Arabidopsis complementation
AtSGR1_promoter-R	AACTACACATCTCTGCTTGAAACC CA	Arabidopsis complementation
AtSGR_CrSGR-F	GAGAGCAGAGATGTGTAGTTTGTC GGCGAT	Arabidopsis complementation
CrSGR_pENT-R	AAGCTGGGTCTAGATTCACTTGTC GTCATCGTCTT	Arabidopsis complementation
AtTransit_pENT-F	GCAGGCTCCACCATGTGTAGTTTG TCGGCGATTAT	Arabidopsis complementation
CrSGR_T-F	TGAGGAGGACCAGCAGCAAC	Arabidopsis complementation
CrSGR_T-R	GAACCGAAACCGGCGGTAAG	Arabidopsis complementation
ACT2-F	AGTGTTGTTGGTAGGCCAAG	Arabidopsis complementation
ACT2-R	CAGTAAGGTCACGTCCAGCA	Arabidopsis complementation
CrSGR-F	GGCACAAGTAGCAGCAGTAG	Arabidopsis complementation
CrSGR-R	CACTTGTCGTCATCGTCTTTG	Arabidopsis complementation